Layered Calcium Borohydride Polymorph via an Enhanced Evolutionary Algorithm

Vladimir Baturin, Jean-Claude Crivello

Layered Calcium Borohydride Polymorph via an Enhanced Evolutionary Algorithm

Vladimir Baturin*,† and Jean-Claude Crivello*,†,‡

†*Université Paris Est Créteil, CNRS UMR 7182, ICMPE, F-94010 Créteil, France*

‡*CNRS-Saint-Gobain-NIMS, IRL 3629, Laboratory for Innovative Key Materials and Structures (LINK), 1–1 Namiki, 305–0044 Tsukuba, Japan*

E-mail: vladimir.s.baturin@gmail.com; jean-claude.crivello@cnrs.fr

Abstract

Complex hydrides are attracting increasing attention as promising solid hydrogen storage materials, yet theoretically exploring their chemical space is a challenging task due to their often intricate structures. In this work, we present an improved evolutionary crystal structure prediction method tailored to systems with rigid building blocks, enabling a reduction in search space dimensionality without losing relevant solutions and significantly speeding up the search. The developed method was validated by successfully reproducing the known structures of borohydrides and alanates of lithium, sodium, and potassium, while also revising their vibrational and energetic properties. Furthermore, this approach, together with in-depth phonon analysis, led to the prediction of a new metastable $P\bar{3}cm$ phase of $Ca(BH_4)_2$, only 1.5 meV/atom above the known ground state. This phase exhibits a layered geometry unusual for complex hydrides, combining covalent, ionic, and van der Waals bonding, with the potential for both chemical and physical hydrogen storage via intercalation.

Keywords

Complex hydrides, two-dimensional materials, hydrogen storage, structure prediction, evolutionary algorithm, electronic structure calculation

1 Introduction

One of the major challenges of the 21st century is the generation and utilisation of non-polluting energy.[1] Hydrogen, with its high energy density and clean combustion products, is an ideal energy carrier for applications such as mobile devices, transportation, and stationary energy storage.[2] However, efficient and safe hydrogen storage remains a critical hurdle in the development of a hydrogen-based economy.[3,4]

Among the various hydrogen storage methods, materials based on hydrides offer significant advantages over traditional approaches such as tanks with compressed or cryogenic liquid hydrogen.[5] They have played a pivotal role in advancing practical energy storage technologies, with nickel–metal hydride batteries being the most prominent example.[6] In metal hydrides, MH, hydrogen is stored in atomic form within the interstitial sites of the crystal lattice. These materials initially garnered significant attention due to their reversibility, rapid kinetics near room temperature, and high volumetric hydrogen uptake, comparable to that of liquid hydrogen. Recent research has focused on improving the hydrogenation properties of these materials for dedicated applications such as superconductivity at ambient conditions.[7] However, their low gravimetric hydrogen densities as compared to high-pressure tank systems have led to a shift in research interest toward other storage systems in the past decade, e.g. carbon-based materials, metal-organic frameworks and promising complex-anion metal hydrides.

These latter compounds have excellent gravimetric and volumetric capacities that outperform most other materials.[8] They are typically represented as ${M^{m+}}_n[T\mathrm{H}_x]^{n-}{}_m$, where M^{m+} is a metal cation (alkali, alkaline earth, or transition metals) and $[T\mathrm{H}_x]^{n-}$ is a hydrogen-

containing anionic unit, with hydrogen atoms covalently bonded to the central atom T, such as aluminum, boron, or nitrogen. Therefore, the hydrogen in these structures is partially charged and localized, contributing to the unique properties of these materials.[9]

One of the first families of complex hydrides to be extensively studied, due to its high storage capacities, is the alanates which are based on aluminum, as the T element. In the late 90s, these materials gained significant attention due to their potential for reversible storage. Contrary to the prevailing belief that complete anions were too strongly bound and thus hindering the reversibility, Bogdanovic *et al.* demonstrated that hydrogen could be reversibly extracted from alanates through a two-step reaction, enabled by doping the material with a small amount (a few mol%) of titanium.[10] Derived from aluminum hydride (AlH_3), a covalently bonded polymorph that is thermodynamically unstable at room temperature, complex alanates exhibit greater stability. This is because the covalently bonded Al–H complex exists as an anion (*e.g.*, AlH_4^-, AlH_6^{3-}) that is stabilized by a metal cation. Alanates can exist in several main forms, notably tetrahydroaluminates, $M^{m+}[AlH_4^-]_m$, where aluminum is tetrahedrally coordinated by hydrogen, and hexahydroaluminates, $M^+_{3n}[AlH_6^{3-}]_n$, where aluminum is octahedrally coordinated.[11]

Among other families of complex hydrides, metal borohydrides, where boron and hydrogen form negatively charged BH_4^- anions counterbalanced by metal cations, have been extensively studied for their potential in hydrogen storage.[12] The first homoleptic metal borohydrides, $Al(BH_4)_3$, $Be(BH_4)_2$, and $LiBH_4$, were discovered as early as 1940, although the crystal structure of this latter or a more complex ones, such as $Mg(BH_4)_2$, were only resolved much later[13,14]. Recent advances have also highlighted the potential of complex hydrides as solid-state electrolytes in batteries.[15,16]

In the case of complexes of transition metal hydrides, the bonding flexibility with hydrogen introduces a variety of interesting functionalities. Several studies have demonstrated the benefits of this flexibility, with particular focus on the role of electronegativity in explaining the diverse cohesion mechanisms observed in these hydrides.[17] For a comprehensive

review of transition metal hydrides and their well-known structures, further reading is recommended.[18] Intense interest has developed in other low weight complex hydrides[19] such as amides $[NH_2]^-$,[20] or amidoboranes.[21] However, strong iono-covalent complexes, such as boranes, are known to be stable and only decompose at elevated temperatures, yet they still have other properties interesting for applications such as colossal barocaloric effects in complex Li–B–H compounds.[22]

The discovery of new, more efficient hydrogen storage materials is a formidable challenge due to the vast complexity of potential phases. Although experimental methods provided a number of important results, they are often limited in scope and expensive when exploring the broad landscape of possible compositions. Consequently, theoretical prediction methods have gained prominence as a valuable alternative.

When a comprehensive database of materials with similar properties is available, high-throughput combinatorial screening becomes the method of choice. Coupled with electronic structure calculations to estimate the energies of sampled compounds,[9,23] this approach has proven to be a powerful tool for identifying stable atomic configurations within known prototype phases.[24–27] In the context of complex hydrides we note a comprehensive review of structural mapping between homoleptic metal borohydrides and their structural prototypes.[28]

However, despite its efficiency, even when enhanced by supervised machine learning algorithms,[29–31] combinatorial screening is inherently limited to known structural prototypes, making it less effective for discovering completely new phases. To push beyond these boundaries, evolutionary and generative methods offer a more promising approach for identifying truly novel materials.

First, we mention the Prediction by Electrostatic Ground State (PEGS) search method, which has been applied to produce ground-state structures for complex hydrides such as $NaAlH_4$, $Mg(AlH_4)_2$, and the mixed-cation alanate K_2LiAlH_6.[32] This approach leverages two key observations: (i) The structures of complex metal hydrides are characterized by

an arrangement of positively charged cations (*e.g.* Na^+) and negatively charged complex anions (*e.g.* AlH_4^-), where strong covalent bonds within the anions can be treated as rigid units. This reduces the number of free variables, thereby increasing search efficiency. (ii) Interactions between cations and anions are dominated by electrostatics, modeled using a simple Hamiltonian as a function of inverse distances. However, as illustrated below in our study, the bonding pattern in complex hydrides often goes essentially beyond electrostatics – a possible reason why some of the PEGS predictions[9] have no experimental backup.

Moreover, genetic algorithms have also been applied to search for new metal hydrides, particularly in the field of superconducting hydrogen compounds. For example, this method predicted hypothetical ternary hydrogen compounds, such as $KScH_{12}$, which features a modulated hydrogen cage and exhibits a superconducting critical temperature of 122 K at 300 GPa. Another example is $GaAsH_6$, which was predicted to show superconductivity at 98 K under 180 GPa.[33]

Nowadays, a rapidly evolving approach is the generative method based on statistical learning, including neural networks. One example is the first generative adversarial network applied to crystal structures, specifically metal hydrides, called CrystalGAN.[34] However, it was limited since no energy criterion was used as a validation method. Recently, denoising or diffusion models became the state-of-the-art for images generation and now, using graph neural networks as descriptors for crystals, they are being applied to materials discovery.[35,36] For example, score-based approaches on two separated networks (one for lattice, one for atoms position) have demonstrated the ability to generate new stable structures.[37,38] However, they are still limited when dealing with a large degree of freedom, such as the number of non-equivalent sites or different elements.

Despite the drastic development of the ML-based generative methods of crystal structure prediction, currently among the most robust tools are the evolutionary[39–41] and swarm intelligence[42] approaches. These methods are inspired by the natural processes, survival of the fittest and collective foraging correspondingly. They allowed to discover a vast num-

bers of new materials, from new phases of already known compounds[43] to unexpected low-dimensional materials[44] to a series of hydrogen-rich materials[45] relevant to the hydrogen storage field.

In this work we explore the chemical space of complex hydrides of $M^{m+}{}_n[T\mathrm{H}_x]^{n-}{}_m$ formula using the evolutionary algorithm based on the USPEX code[40] that we improve to efficiently target these materials. Namely, we harness the fact that T and H atoms almost certainly form rigid structural motifs (BH_4 tetrahedra *etc.*). Using them as structural units effectively reduces the search space dimensionality thus accelerating the search and permits accessing larger systems. The latter is important since many complex hydrides are notorious for their structural complexity. The paper is organized as follows: first, we explain the computational context and show the new developments to the evolutionary algorithm, then we move on to the validation part, where we reproduce the known borohydrides $M\mathrm{BH}_4$ and alanates $M\mathrm{AlH}_4$ of three first alkali metals M, providing also the analysis of their enthalpy of formation with vibrational contribution taken into account. Finally, we apply our method to $\mathrm{Ca(BH_4)_2}$ and demonstrate that along with a well-known *Fddd* ground state, there is a new metastable phase which is only 1.5 meV/atom higher in energy and has an unexpected layered morphology.

2 Computational methods

2.1 Crystal structure prediction

The evolutionary Crystal Structure Prediction (CSP) was conducted using the USPEX code,[39,40,46,47] where we upgraded the module responsible for handling complex building blocks (specifically, complex anions). These refinements are discussed in detail in the Results section. Otherwise the evolutionary search followed standard routines, starting with the creation of the initial generation: 250 trial structures constructed using random symmetry and random topology[48]-based methods. Then the structures are locally optimized at

the DFT level and the final energy is used to evaluate the fitness of structures (see below). Subsequent generations, each containing 100–150 structures, were partially derived from the parent generation through crossover and mutation operators, and partially consisted of yet again randomly generated candidates to balance exploration and exploitation. As with the initial generation, each structure is evaluated through DFT relaxation to minimize the residual forces. The search was considered converged if no new best structures emerged over 20 consecutive generations. Typically, finding the best structure required 10–50 generations.

2.2 First principle calculations

Various configurations of first-principles calculations were utilized in our research, all by means of DFT using Vienna Ab Initio Simulation Package[49,50] (VASP). During the CSP, each candidate structure underwent a four-step local geometry optimization as follows. *Step 1*: ionic positions optimization with a fixed cell, *step 2*: volume optimization with fixed shape and fractional ionic coordinates, *step 3*: cell shape optimization and, finally, *step 4*: full relaxation. For step 4, we used Perdew-Burke-Ernzerhof[51] (PBE) gradient-corrected exchange and correlation functional, a plane wave basis set with an energy cutoff of 600 eV and a Γ-centered Monkhorst-Pack k-mesh[52] with a resolution of k-points of $0.03\times2\pi/\text{Å}$ in each direction. The Self-Consistent Field (SCF) electronic cycle and geometry optimization were performed until the difference of electronic energy ΔE_{SCF} and maximum force acting on atom F_{max} were below 10^{-6} eV and 10^{-5} eV/Å correspondingly. These settings are rather loose since the CSP screens thousands of structures. For the final refinement and subsequent phonon calculations we selected 10 best geometries for each composition and performed the high-accuracy relaxation with 750 eV energy cutoff, twice denser k-point mesh (verified by convergence tests), and using the rev-vdW-DF2 non-local van-der-Waals approach,[53] recently suggested[54] as most suitable for layered structures, which were found in abundance during the evolutionary search. The ΔE_{SCF} and F_{max} were lowered to 10^{-9} eV and 10^{-8} eV/Å correspondingly. The phonon dispersion curves and zero point energy (ZPE) were calculated

using Phonopy software[55,56] coupled with VASP (same DFT settings as for the fine relaxation). Finally, to calculate electronic band structure, the HSE06[57] hybrid functional was utilized. Bader charges were estimated using Henkelman group's algorithm.[58]

3 Results and discussion

3.1 Guided evolutionary CSP

The computational search for new materials requires finding the global optimum (GO) of a fitness function F over atomic configuration space. For optimizing stability, F is typically energy, enthalpy, or another thermodynamic function. Success in finding the GO depends on the algorithm's quality (Q) and the search space dimensionality d. This can be conceptually expressed by the time required to find the GO: $T_{\mathrm{GO}} \sim Q \exp(\lambda(Q) \cdot d)$, where $\lambda(Q)$ is a function of Q. While much effort is put into improving algorithm efficiency, reducing d must be done carefully to avoid missing any important solutions. In a way, the art of efficient search is to perfectly set up the constraints based on all available information about the sought solution. In complex hydrides ${M^{m+}}_n[T\mathrm{H}_x]^{n-}{}_m$, such a reduction is possible by considering anions $T\mathrm{H}_x$ as rigid units. Hence, instead of optimizing $x+1$ independent atoms (*i.e.* $3(x+1)$ spatial variables), one needs to optimize the position of the anion as a whole (6 variables: position of the center and orientation).

In this work, the main tool for exploring the chemical space of complex hydrides is the Evolutionary Algorithm (EA) USPEX. The algorithm converges to the optimal solution by: (1) Creating an initial random set of structures (first generation); (2) Evaluating them by performing local optimization using third-party codes; (3) Discarding a certain percentage of the worst structures and using the remaining "individuals" as parents; (4) Creating the new generation by applying variational operators, such as cross-over (heredity) and mutations. This process repeats until the convergence criteria are met.

Besides being well-established for its efficiency in finding optimal positions of atoms,

USPEX has the functionality of using complex molecular units as building blocks.[47] Not only does it build trial structures from complex units, but it also monitors their integrity, which can be disrupted during relaxation or by the application of variational operators. Such control reduces wasted computational time and prevents convergence to more stable structures where the structural units are dismantled, a situation common in metastable organic crystals.

We have reviewed and improved this monitoring process. First, we implemented automatic generation and tracking of bond graphs within blocks, which helps to filter out structures that become heavily deformed during relaxation. Secondly, we identified and fixed the following rather hidden issue. The crossover operator slices parent structures and combines slabs from different parents to form an offspring. To prevent cutting through a building block, USPEX checks the position of the block's center of mass relative to the cutting plane and either includes the entire block or excludes it completely (Figure 1a), regardless of the positions of constituent atoms. The important point here is that this determination is done in Cartesian coordinates. If, during relaxation, an atom of the block crosses the unit cell boundary, it is replaced by its periodic image *within* ("wrapped into") the cell. While this doesn't change the system physically, it destroys the unit's integrity in *Cartesian* coordinates, leading to malfunction of the crossover operator. We detect and fix such situations through a process we call "dewrapping" (Figure 1b).

In previous USPEX versions, this problem was addressed by subtracting the rounded values from fractional coordinates, *e.g.* toggling a wrapped 0.95 fractional coordinate back to $0.95 - \mathrm{round}(0.95) = -0.05$, which often worked, but failed when the size of the structural unit was comparable to the cell dimension. This is the case with the alanate anion AlH_4^- considered in this work. We developed a more reliable procedure that scans all distances in Cartesian space and, when a change is detected, checks all nearest periodic images to restore the initial distances within a given error threshold.

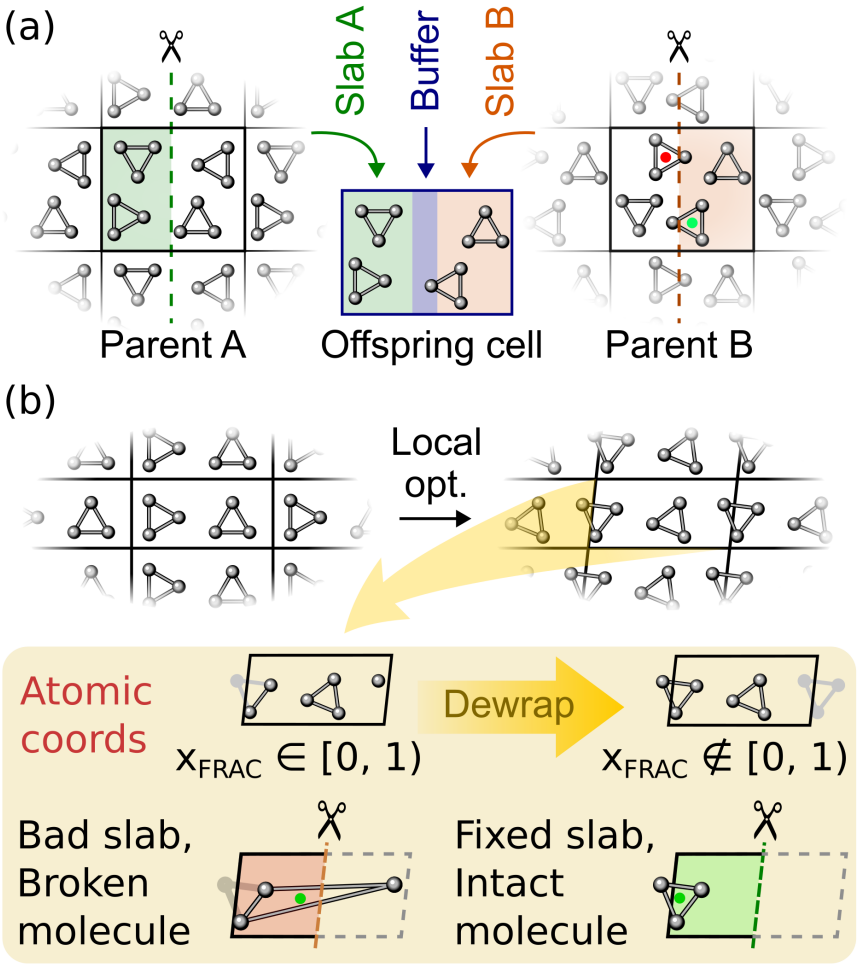

Figure 1: (a) Crossover operator in a nutshell. Green and red dots denote centers of mass of molecules that happened to be within and outside a slab, correspondingly. (b) Consequences of internal wrapping of all fractional coordinates into $[0, 1)$ interval and correcting them by the dewrapping procedure.

3.2 Validation of Guided CSP

To ensure the workflow yields accurate results, we conducted an evolutionary search to reproduce stable structures of known borohydrides and alanates of first three alkali elements in the form of MTH_4, where $M = \{\text{Li, Na, K}\}$ and $T = \{\text{B, Al}\}$ with metal cation and TH_4 anions used as building blocks as described above.

As noted in the computational technique section, the DFT parameters used during the CSP search offer moderate precision, leaving the true global minimum within $\sim 10\,\text{meV/atom}$ above the CSP solution. To address this, we reoptimised all pertinent candidate structures within this range using high-precision parameters. Additionally, we performed a phonon study of the most promising structures to refine their corrected enthalpy of formation (by adding the corresponding ZPE correction) and to verify their dynamical stability.

For all six target MTH_4 compounds, we identified either the previously known global optimum or one of several known nearly degenerate low-energy phases. It took a few thousand EA candidates to find a solution for each MTH_4 formula. Resulting structures are presented in Fig. 2 and their structural parameters can be found in Table 1.

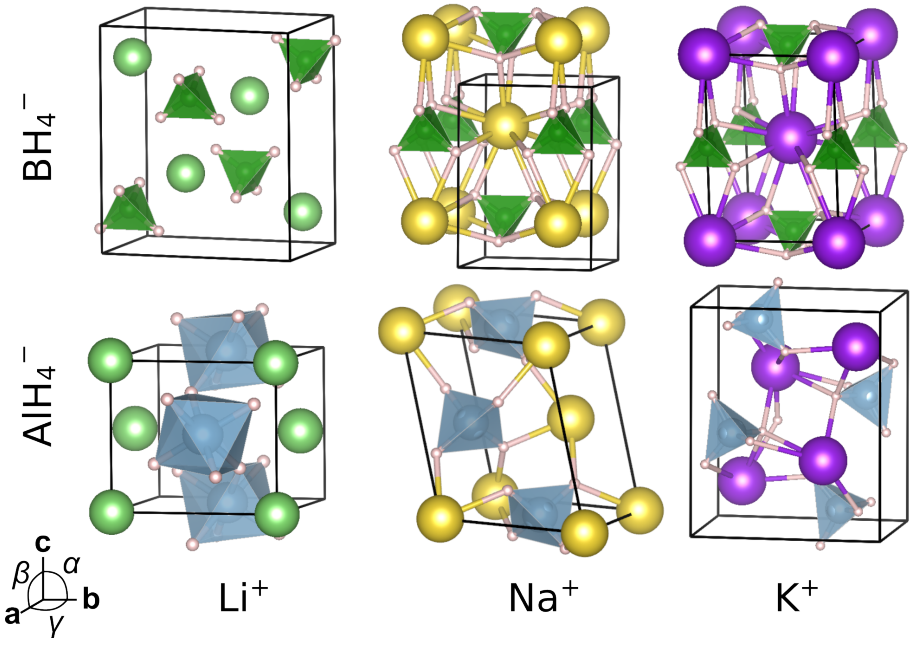

Figure 2: Reproduced structures for borohydrides and alanates of three first alkali metals.

Table 1: Space group (SG); cell parameters (*cf.* frame in Figure 2): lengths (a, b, c, in Å) and angles (α, β, γ, in 1°); volume per formula unit (V_{fu}, Å^3) for borohydrides and alanates of Li, Na and K.

Formula	$LiBH_4$	$NaBH_4$	KBH_4	$LiAlH_4$	$NaAlH_4$	$KAlH_4$
SG	$Pnma$	$P4_2/nmc$	$P4_2/nmc$	$Pnc2$	$I4_1/a$	$Pnma$
a	4.38	4.36	4.75	5.10	5.00	5.81
b	6.50	4.36	4.75	4.74	5.00	7.38
c	7.48	5.89	6.68	4.21	6.59	8.91
α	90.00	90.00	90.00	90.00	112.29	90.00
β	90.00	90.00	90.00	90.00	112.29	90.00
γ	90.00	90.00	90.00	90.00	90.00	90.00
V_{fu}	106.49	55.97	75.60	50.97	69.61	95.62

The electronic band structures of these materials are not discussed in this paper since they have been extensively described in previous works:[23,59,60] in all cases the T- and H orbitals overlap in the valence band which indicate the covalent bonding within the $[TH_x]^-$ anion, while its interaction with M^+ cation is ionic. The latter can be illustrated from Bader analysis, which we carried out for $LiBH_4$, showing that the Li^+ and $BH_4{}^-$ have absolute charges of $0.89|e|$. The degeneracy of the polymorphs, discovered by our approach for the same chemical target, can be explained by their phonon spectra and the corresponding Density of States (DOS). A typical example is $LiBH_4$, shown in Figure 3a. Three distinct bands are observed: the two higher bands correspond to intramolecular bending and stretching vibrations of the BH_4 complex, while the lower band consists of soft inter-ionic modes, resulting in a smooth potential energy surface and many shallow low-energy minima.

This behavior is observed in all of the considered compounds, except for a peculiar case: the *Pnc2* phase of $LiAlH_4$. Building the initial structures from AlH_4 tetrahedra, the evolutionary search ended up with a solution containing hydrogen sharing AlH_6 octahedra, a previously known high-density γ-$LiAlH_4$ polymorph.[61] The increased connectivity is reflected in the broader phonon bands (Figure 3b). This transformation occurred because our method permits controlled deformations of structural units, specifically allowing up to a 10% relative variation in interatomic distances during relaxation stages, thus demonstrating how the

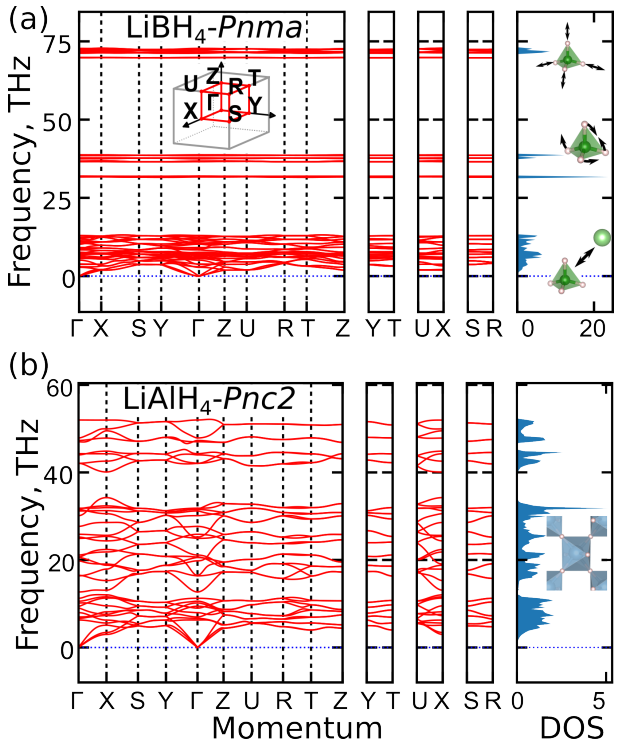

Figure 3: Phonon dispersion curves and density of phononic states of (a) $LiBH_4$ in *Pnma*: three bands well-separated by gaps typical for all found structures except for $LiAlH_4$, and (b) $LiAlH_4$ in *Pnc*2. Brillouin zone and high-symmetry paths, common for both structures are shown within the first panel. Projected DOS subpanels contain characteristic structural motifs responsible for corresponding bands.

flexibility of the approach enables the efficient discovery of improved configurations that might be overlooked when strictly rigid building blocks are used. The ability to understand and track these structural transformations is what makes our method transparent – a feature often lacking in neural network-based prediction methods.

Using the obtained data we also provide the energies of formation at 0 K, with and without the ZPE correction. The values are calculated with respect to pure substances, the bcc structures of Li, Na and K, α-phase of boron, fcc-Al and H_2 gas. The Table 2 sums up the results alongside the available experimental data.

Table 2: Energies of formation at 0K without ($\Delta_f H^0_{\mathrm{DFT}}(0K)$) and with ($\Delta_f H^0_{\mathrm{DFT+ZPE}}(0K)$) ZPE, value of ZPE correction δ_{ZPE}, experimental value at 298 K if available, kJ/mol.

Compound	$\Delta_f H^0_{\mathrm{DFT}}(0K)$	δ_{ZPE}	$\Delta_f H^0_{\mathrm{DFT+ZPE}}(0K)$	Exp.
$LiBH_4$-$Pnma$	-196.43	40.10	-156.3	-194.46[62]
$NaBH_4$-$P4_2/nmc$	-189.58	38.47	-151.11	-191.84[62]
KBH_4-$P4_2/nmc$	-230.51	37.17	-193.33	-228.86[62]
$LiAlH_4$-$Pnc2$	-92.56	28.01	-64.55	-117.15[62]
$LiAlH_4$-$P12_1/c1$	-85.19	22.98	-62.21	—
$NaAlH_4$-$I4_1/a$	-79.29	22.11	-57.18	-112.97[63]
$KAlH_4$-$Pnma$	-116.30	17.48	-98.82	-166.52[63]

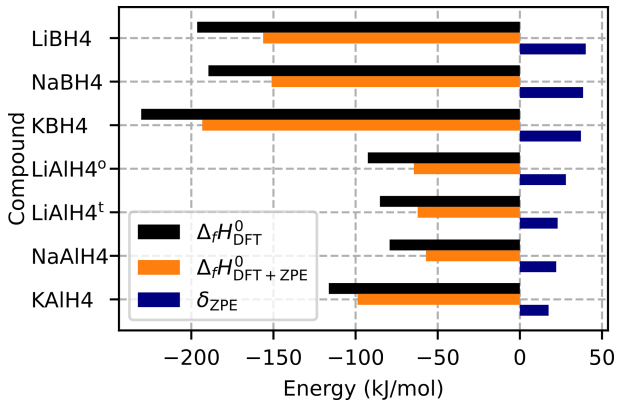

Figure 4: ZPE effect on formation enthalpy. LiAlH4° LiAlH4ᵗ stand for octahedra and tetrahedra-based polymorphs ($Pnc2$ and $P12_1/c1$ correspondingly).

The corresponding values are shown in Figure 4. Notably, the uncorrected values show better agreement with measured data than those corrected with ZPE. This phenomenon was observed before, and the reason of it remains unclear.[59,64] It is important to keep in mind that

our methodology relies on the harmonic approximation, neglecting anharmonic contributions. Nonetheless, the ZPE contribution remains significant, as vibrational effects destabilize the system (with a sign opposite to chemical energy), accounting for approximately 20% of the formation enthalpy value (as observed for $LiBH_4$). We also included the values for a low energy $P12_1/c1$ polymorph of $LiAlH_4$ with separate tetrahedral AlH_4 complexes. This structure has a reduced δ_{ZPE} consistent with its less connected loose structure compared to the octahedral network in $Pnc2$ polymorph. The corresponding dispersion curves can be found in Table S1 in Supporting Information (SI).

3.3 Novel layered polymorph of $Ca(BH_4)_2$

The main result of this study was obtained as a logical continuation of the validation procedure. Unlike the structures considered above with 12-24 atoms, the borohydrides and alanates of alkaline earth metals have much more complicated structures (88 and 132 atoms in primitive cells of borohydrides of Be and Mg respectivly), and reproducing these structures would make a computationally very costly study on its own. Putting these two challenging compounds aside, we launched the evolutionary search of the $Ca(BH_4)_2$ structure. As before, the objective was to reproduce the previously known ground state, or, in this case, the α-phase. However, identifying a suitable reference proved challenging, as multiple competing structural models have been proposed over the years. Early work by Miwa *et al.*,[65] based on X-ray diffraction (XRD) and ab initio studies, suggested an $Fddd$ symmetry. Later, Filinchuk *et al.*,[14] using advanced in situ synchrotron measurements, put forward the $F2dd$ space group and identified a high-temperature α'-phase with $I\bar{4}2d$ symmetry, a supergroup of $F2dd$. Soon afterward, Majzoub *et al.*[66] combined XRD and ab initio calculations involving phonons study to find that at 0 K the $Fddd$, $F2dd$, and newly proposed $C2/c$ structure (also denoted as α-phase) are essentially isoenergetic. This structural diversity can be explained by the sensitivity of the material to synthesis conditions.[66] Yet we note that, despite these variations, all proposed α-phases share the same fundamental structural motif: parallel

Ca-sharing layers composed of $[=(CaBH_4)_2=]_\infty$ ribbons, with the ribbons in adjacent layers oriented nearly perpendicularly (see Figure 5A). Differences among the proposed structures lie mainly in the relative orientations of BH_4 tetrahedra and subtle unit-cell distortions, but this underlying motif holds the same. It is precisely this common structural backbone that we aimed to recapture with our predictive approach. The corresponding orthorombic structure with $Fddd$ symmetry and cell parameters of $8.75 \times 13.13 \times 7.50$ Å was found after about 20 generations, totaling to 3000 candidate structures proposed and screened by the USPEX. Figure 5 shows the ground state together with metastable polymorphs proposed by the evolutionary algorithm within the 10 meV range above the solution.

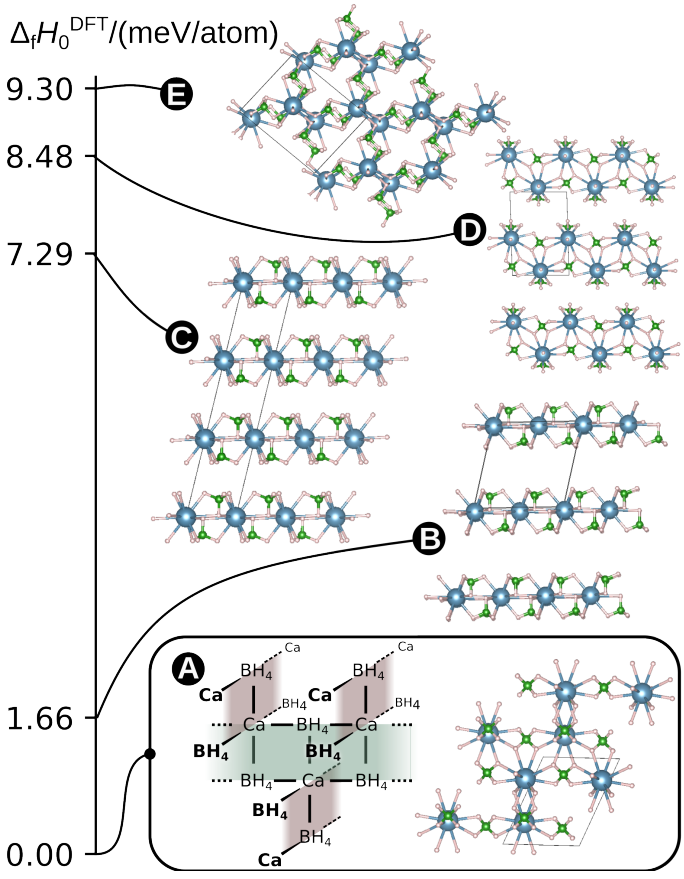

Figure 5: Optimum $Ca(BH_4)_2$ structure and its polymorphs within 10 meV/atom above it as obtained from the global optimization. A: previously known α-phase: an arrangement valid for all suggested symmetries and an $Fddd$ variant found in our evolutionary search; B: New phase of trigonal layers; C: Underrelaxed version of B; D: Layered phase containing motifs of $Fddd$; E: $P1$ structure, slightly denser than $Fddd$. Enthalpies of formation are shifted by that of $Fddd$ phase equal to -356 meV/atom (in DFT setting used in USPEX).

Among higher lying trial solutions we also found various distorted versions of β-$Ca(BH_4)_2$ phase. It is important to note here that the method is not aimed to identify *all* low-energy metastable phases, but is designed to find the global minimum. Nevertheless, to our surprise, the search revealed a variety of low-energy structures having layered arrangement. The most stable among them (Figure 5B) is remarkably only 1.66 meV/atom higher than the ground state, according to moderate-precision DFT procedure for CSP. Two other 2d structures are: C, an underrelaxed version of B, and D, a more complex bilayered polymorph, which combines the two-dimensional morphology with reticular topology inherent to borohydrides of alkaline earth metals (one can see the motifs resembling the $Fddd$ structure). The next refinement step with increased DFT accuracy and inclusion of advanced dispersion correction confirmed that the lowest metastable polymorph indeed consists of layers, similar to structure B, but the sheets are stacked without shifting and are separated by 2.5 Å-thick layer of vacuum (Figure 6). The space group of the structure is $P\bar{3}m1$. The motif can be described as follows: the BH_4^- anions form a nearly octahedral coordination of the Ca_2^+ cations with a face of octahedra parallel to the layer plane. All six anion tetrahedra point towards the layer plane. These motifs arrange into layers through triangular tiling. The obtained layered structure is unprecedented in homoleptical complex hydrides but has been identified in an anion-ordered iodine-substituted compound, $Ca(BH_4)_{1.40}I_{0.60}$.[67]

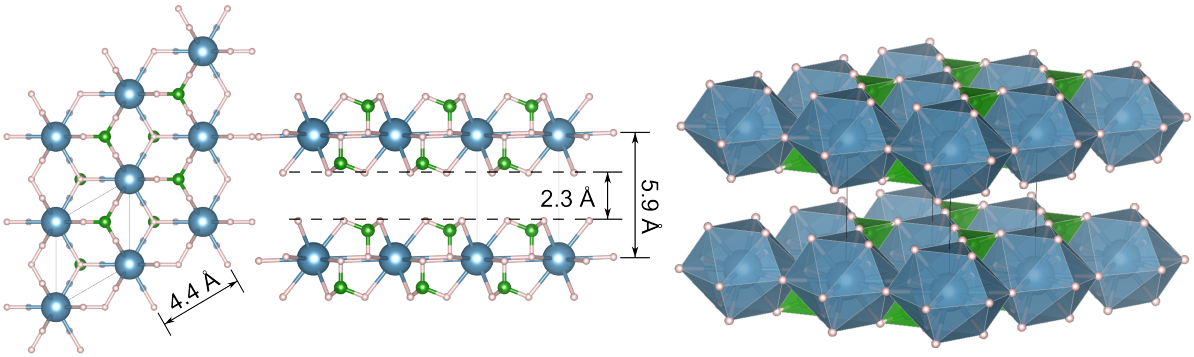

Figure 6: Layered polymorph of $Ca(BH_4)_2$: top, side and coordinational polyhedra views.

To assess the dynamic stability of this phase, we computed the phonon spectrum and

found imaginary vibration modes along the $\Gamma - A$ segment (Figure 7, left panel). Given the small magnitude of these imaginary frequencies, these modes are "soft", *i.e.* the corresponding motion implies low change in energy. With this in mind, we explored various layer stacking arrangements, but consistently observed imaginary frequencies in each configuration (See SI, Table S2).

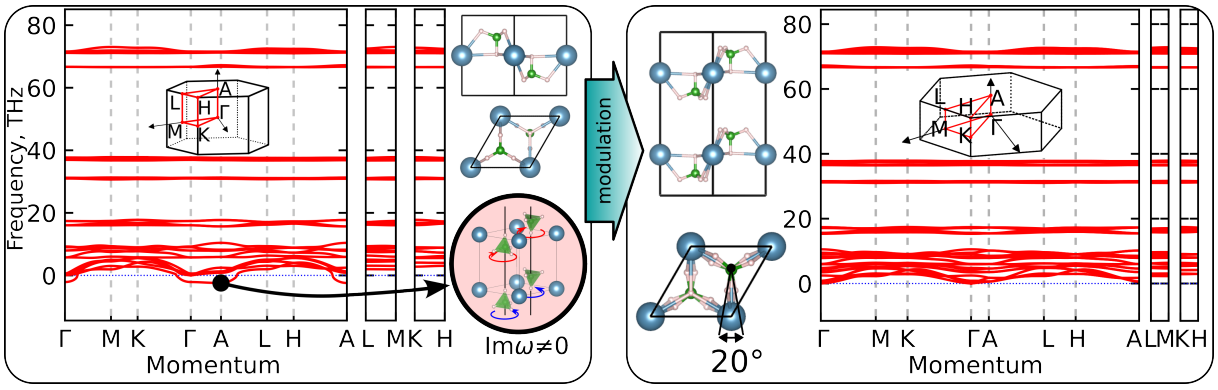

Figure 7: Analysis of dynamic stability of layered structure: imaginary modes related to twisting vibrations of BH_4^- tetrahedra (left panel) lead to an idea of stabilisation by distorting the structure along the mode with highest absolute value (antiphase twisting). The resulting structure with doubled unit cell is indeed dynamically stable (right panel).

Consequently, we decided to directly examine the collective motion associated with these imaginary modes. It turned out to be a twisting of tetrahedral motifs, in-phase within a layer, and having a interlayer phase difference in adjacent layers from 0 (Γ-point in the Brillouin zone) to π (point A, see the circle inset in Figure 7). Since an imaginary frequency in the equilibrium structure indicates a saddle point, we hypothesized that displacing or modulating the structure in this direction might lead it to a lower, true local minimum. This hypothesis was confirmed: by following this path, the corresponding structure indeed relaxed into a more stable configuration with no imaginary frequencies. The new geometry has the tetrahedra in adjacent layers BH_4^- twisted by 20° around a normal to the layers (Figure 7, right panel). Due to the doubling of period the symmetry of structure was lowered to $P\bar{3}c1$. The enthalpy of formation with the ZPE correction is -281.2 meV/atom, or -149 kJ/mol BH_4. As a reference, the corresponding value for $Fddd$ phase $\Delta_f H(0\,\mathrm{K}) = -282.7$ meV/atom or -150 kJ/mol BH4, which agrees with previous studies.[65]

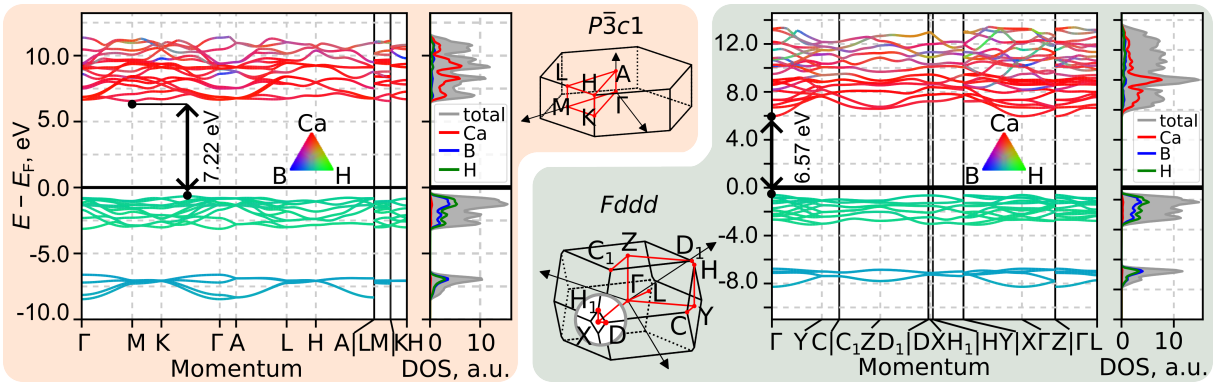

Figure 8: Electronic bands dispersion curves and integrated density of states of $Ca(BH_4)_2$ in the layered $P\bar{3}c1$ compared to the known $Fddd$ phase.

To better understand the new phase, particularly its bonding pattern, we calculated its electronic dispersion curves (using the HSE06 hybrid functional with rev-vdW-DF2 dispersion correction), Bader charges, and exfoliation energy. As shown in Figure 8, the layered candidate is an indirect insulator with a band gap of 7.22 eV which is larger than 6.57 eV direct gap in $Fddd$. The projected DOS reveals significant overlap between the B and H orbitals in the valence band, indicating predominantly covalent bonding within the anions, likely due to the σ-coupling of hydrogen's s-orbitals with the sp^3-hybridized orbitals of boron. However, Bader charges of $+1.95|e|$ for B and -0.68$|e|$ for H suggest a potentially mixed ionic-covalent character, a point that's debated in earlier literature.[59] The interaction between the anions and Ca cations, on the other hand, is clearly ionic, as we observe no orbital overlap, and the Bader charges on Ca are $+1.55|e|$. The exfoliation energy, calculated as the energy difference between a per-layer energy of the phase and that of an isolated single layer, was determined using a supercell approach. The layers were separated by 20 Å of vacuum to avoid interaction between periodic images. The resulting exfoliation energy is -190 meV per formula unit, or -11.5 meV/Å^2, which is about three times lower than that of graphite.

4 Conclusions

We applied an evolutionary approach to explore the chemical space of complex hydrides ${M^{m+}}_n[T\mathrm{H}_x]^{n-}{}_m$, optimizing the crystal structure composed of discrete blocks—specifically complex anions—rather than individual atoms. While this mode had been introduced before,[47] it required several key refinements to function effectively for such systems. After implementing these improvements, the method was validated and has been shown to reliably predict crystal structures from given building blocks, providing a powerful tool for exploring complex hydrides in the context of hydrogen storage applications. During the validation of the methodology, the known borohydrides and alanates of three first alkali metals were reproduced and their energies of formation revisited with vibrational contributions taken into account. The new method, assisted by in-depth phonons study allowed to predict the new unexpected low-energy metastable phase of $\mathrm{Ca(BH_4)_2}$ with a layered geometry of $P\bar{3}c1$ space group, only 1.5 meV/atom higher than the known $Fddd$ structure. The new material has a three-tiered bonding scheme. At the first level, the complex $\mathrm{BH_4}^-$ anions are formed through strong covalent bonds, providing a means of chemically storing hydrogen within the structure. At the second level, these anionic complexes interact with calcium cations via ionic bonding, resulting in stable two-dimensional layers. Finally, at the third level, the layers are held together by weak van der Waals forces, allowing for flexibility between them. This opens up the possibility not only for chemical hydrogen storage via the $\mathrm{BH_4}^-$ anions but also for hydrogen absorption between the layers. While the material's potential for intercalation-based hydrogen storage requires further study, this combination of chemical and possible physical absorption mechanisms makes it a promising candidate for hydrogen storage applications, with potential relevance for energy technologies where reversible gas absorption and release are essential. As other layered materials, the new phase is worth studying in many other aspects related to its optical properties, possible battery applications, *etc.*

Acknowledgement

This work is a part of project PEPRH2-SOLHYD (ref. ANR-22-PEHY-0007) funded and supported by the French National Research Agency (ANR) under the France 2030 program. DFT calculations were performed using HPC resources of GENCI–CINES (Grant A0060906175). VB thanks Pavel Bushlanov for his invaluable help and guidance in coding.

Supporting Information Available

- Table S1: Phonon dispersion curves of borohydrures and alanates of Li, Na, K, reproduced by evolutionary search;
- Table S2: Phonon dispersion curves of different stacking of $P\bar{3}m1$ structure.

References

(1) Winter, C.-J. Hydrogen energy — Abundant, efficient, clean: A debate over the energy-system-of-change. Int. J. Hydrogen Energy **2009**, 34, S1–S52.

(2) Schlapbach, L.; Züttel, A. Hydrogen-storage materials for mobile applications. Nature **2001**, 414, 353–358, Publisher: Nature Publishing Group.

(3) Sandrock, G. A panoramic overview of hydrogen storage alloys from a gas reaction point of view. J. Alloys Compd. **1999**, 293-295, 877–888.

(4) Mohtadi, R.; Orimo, S.-i. The renaissance of hydrides as energy materials. Nat. Rev. Mater. **2016**, 2, 16091.

(5) Hirscher, M.; Yartys, V. A.; Baricco, M.; Bellosta Von Colbe, J.; Blanchard, D.; Bowman, R. C.; Broom, D. P.; Buckley, C. E.; Chang, F.; Chen, P.; Cho, Y. W.; Crivello, J.-C.; Cuevas, F.; David, W. I.; De Jongh, P. E.; Denys, R. V.; Dornheim, M.; Felder-

hoff, M.; Filinchuk, Y.; Froudakis, G. E.; Grant, D. M.; Gray, E. M.; Hauback, B. C.; He, T.; Humphries, T. D.; Jensen, T. R.; Kim, S.; Kojima, Y.; Latroche, M.; Li, H.-W.; Lototskyy, M. V.; Makepeace, J. W.; Møller, K. T.; Naheed, L.; Ngene, P.; Noréus, D.; Nygård, M. M.; Orimo, S.-i.; Paskevicius, M.; Pasquini, L.; Ravnsbæk, D. B.; Veronica Sofianos, M.; Udovic, T. J.; Vegge, T.; Walker, G. S.; Webb, C. J.; Weidenthaler, C.; Zlotea, C. Materials for hydrogen-based energy storage – past, recent progress and future outlook. J. Alloys Compd. **2020**, 827, 153548.

(6) Cuevas, F.; Joubert, J.-M.; Latroche, M.; A. Percheron-Guégan Intermetallic compounds as negative electrodes of Ni/MH batteries. Appl. Phys. A **2001**, 72, 225–238.

(7) Drozdov, A. P.; Eremets, M. I.; Troyan, I. A.; Ksenofontov, V.; Shylin, S. I. Conventional superconductivity at 203 kelvin at high pressures in the sulfur hydride system. Nature **2015**, 525, 73–76.

(8) Modi, P.; Aguey-Zinsou, F. Room Temperature Metal Hydrides for Stationary and Heat Storage Applications: A Review. Front. Energy Res. **2021**, 9, 616115.

(9) Michel, K. J.; Ozoliņš, V. Recent advances in the theory of hydrogen storage in complex metal hydrides. MRS Bulletin **2013**, 38, 462–472.

(10) Bogdanović, B.; Schwickardi, M. Ti-doped alkali metal aluminium hydrides as potential novel reversible hydrogen storage materials1. J. Alloys Compd. **1997**, 253-254, 1–9.

(11) Graetz, J.; Hauback, B. C. Recent developments in aluminum-based hydrides for hydrogen storage. MRS Bulletin **2013**, 38, 473–479.

(12) Paskevicius, M.; Jepsen, L. H.; Schouwink, P.; Černý, R.; Ravnsbæk, D. B.; Filinchuk, Y.; Dornheim, M.; Besenbacher, F.; Jensen, T. R. Metal borohydrides and derivatives – synthesis, structure and properties. Chem. Soc. Rev. **2017**, 46, 1565–1634.

(13) Soulié, J.-P.; Renaudin, G.; Černý, R.; Yvon, K. Lithium boro-hydride $LiBH_4$: I. Crystal structure. J. Alloys Compd. **2002**, 346, 200–205.

(14) Filinchuk, Y.; Černý, R.; Hagemann, H. Insight into $Mg(BH_4)_2$ with Synchrotron X-ray Diffraction: Structure Revision, Crystal Chemistry, and Anomalous Thermal Expansion. Chem. Mater. **2009**, 21, 925–933.

(15) Takahashi, K.; Hattori, K.; Yamazaki, T.; Takada, K.; Matsuo, M.; Orimo, S.; Maekawa, H.; Takamura, H. All-solid-state lithium battery with $LiBH_4$ solid electrolyte. J. Power Sources **2013**, 226, 61–64.

(16) Kim, S.; Oguchi, H.; Toyama, N.; Sato, T.; Takagi, S.; Otomo, T.; Arunkumar, D.; Kuwata, N.; Kawamura, J.; Orimo, S.-i. A complex hydride lithium superionic conductor for high-energy-density all-solid-state lithium metal batteries. Nat. Commun. **2019**, 10, 1081, Publisher: Nature Publishing Group.

(17) Takagi, S.; Iijima, Y.; Sato, T.; Saitoh, H.; Ikeda, K.; Otomo, T.; Miwa, K.; Ikeshoji, T.; Aoki, K.; Orimo, S. True Boundary for the Formation of Homoleptic Transition-Metal Hydride Complexes. Angew. Chem. Int. Ed. **2015**, 54, 5650–5653.

(18) Yvon, K.; Renaudin, G. Hydrides: Solid State Transition Metal Complexes, 2nd ed.; in Encyclopedia of inorganic chemistry; J. Wiley & sons: Chichester, 2005; Vol. III.

(19) Sakintuna, B.; Lamaridarkrim, F.; Hirscher, M. Metal hydride materials for solid hydrogen storage: A review. Int. J. Hydrogen Energy **2007**, 32, 1121–1140.

(20) Chen, P.; Xiong, Z.; Luo, J.; Lin, J.; Tan, K. L. Interaction of hydrogen with metal nitrides and imides. Nature **2002**, 420, 302–304, Publisher: Nature Publishing Group.

(21) Xiong, Z.; Yong, C. K.; Wu, G.; Chen, P.; Shaw, W.; Karkamkar, A.; Autrey, T.; Jones, M. O.; Johnson, S. R.; Edwards, P. P.; David, W. I. F. High-capacity hydrogen storage in lithium and sodium amidoboranes. Nat. Mater. **2008**, 7, 138–141.

(22) Sau, K.; Ikeshoji, T.; Takagi, S.; Orimo, S.-i.; Errandonea, D.; Chu, D.; Cazorla, C. Colossal barocaloric effects in the complex hydride $Li_2B_{12}H_{12}$. Sci. Rep. **2021**, 11, 11915.

(23) Shevlin, S. A.; Guo, Z. X. Density functional theory simulations of complex hydride and carbon-based hydrogen storage materials. Chem. Soc. Rev. **2009**, 38, 211–225.

(24) Hummelshøj, J. S.; Landis, D. D.; Voss, J.; Jiang, T.; Tekin, A.; Bork, N.; Dułak, M.; Mortensen, J. J.; Adamska, L.; Andersin, J.; Baran, J. D.; Barmparis, G. D.; Bell, F.; Bezanilla, A. L.; Bjork, J.; Björketun, M. E.; Bleken, F.; Buchter, F.; Bürkle, M.; Burton, P. D.; Buus, B. B.; Calborean, A.; Calle-Vallejo, F.; Casolo, S.; Chandler, B. D.; Chi, D. H.; Czekaj, I.; Datta, S.; Datye, A.; DeLaRiva, A.; Despoja, V.; Dobrin, S.; Engelund, M.; Ferrighi, L.; Frondelius, P.; Fu, Q.; Fuentes, A.; Fürst, J.; García-Fuente, A.; Gavnholt, J.; Goeke, R.; Gudmundsdottir, S.; Hammond, K. D.; Hansen, H. A.; Hibbitts, D.; Hobi, E.; Howalt, J. G.; Hruby, S. L.; Huth, A.; Isaeva, L.; Jelic, J.; Jensen, I. J. T.; Kacprzak, K. A.; Kelkkanen, A.; Kelsey, D.; Kesanakurthi, D. S.; Kleis, J.; Klüpfel, P. J.; Konstantinov, I.; Korytar, R.; Koskinen, P.; Krishna, C.; Kunkes, E.; Larsen, A. H.; Lastra, J. M. G.; Lin, H.; Lopez-Acevedo, O.; Mantega, M.; Martínez, J. I.; Mesa, I. N.; Mowbray, D. J.; Mýrdal, J. S. G.; Natanzon, Y.; Nistor, A.; Olsen, T.; Park, H.; Pedroza, L. S.; Petzold, V.; Plaisance, C.; Rasmussen, J. A.; Ren, H.; Rizzi, M.; Ronco, A. S.; Rostgaard, C.; Saadi, S.; Salguero, L. A.; Santos, E. J. G.; Schoenhalz, A. L.; Shen, J.; Smedemand, M.; Stausholm-Møller, O. J.; Stibius, M.; Strange, M.; Su, H. B.; Temel, B.; Toftelund, A.; Tripkovic, V.; Vanin, M.; Viswanathan, V.; Vojvodic, A.; Wang, S.; Wellendorff, J.; Thygesen, K. S.; Rossmeisl, J.; Bligaard, T.; Jacobsen, K. W.; Nørskov, J. K.; Vegge, T. Density functional theory based screening of ternary alkali-transition metal borohydrides: A computational material design project. J. Chem. Phys. **2009**, 131, 014101.

(25) Setyawan, W.; Curtarolo, S. High-throughput electronic band structure calculations: Challenges and tools. Comput. Mater. Sci. **2010**, 49, 299–312.

(26) Jain, A.; Ong, S. P.; Hautier, G.; Chen, W.; Richards, W. D.; Dacek, S.; Cholia, S.; Gunter, D.; Skinner, D.; Ceder, G.; Persson, K. A. Commentary: The Materials Project: A materials genome approach to accelerating materials innovation. APL Materials **2013**, 1, 011002.

(27) Kirklin, S.; Saal, J. E.; Meredig, B.; Thompson, A.; Doak, J. W.; Aykol, M.; Rühl, S.; Wolverton, C. The Open Quantum Materials Database (OQMD): assessing the accuracy of DFT formation energies. npj Comput. Mater. **2015**, 1, 15010.

(28) Černý, R.; Schouwink, P. The crystal chemistry of inorganic metal borohydrides and their relation to metal oxides. Acta Crystallogr. Sect. B **2015**, 71, 619–640.

(29) Ong, S. P. Accelerating materials science with high-throughput computations and machine learning. Comput. Mater. Sci. **2019**, 161, 143–150.

(30) Crivello, J.-C.; Joubert, J.-M.; Sokolovska, N. Supervised deep learning prediction of the formation enthalpy of complex phases using a DFT database: The σ- phase as an example. Comput. Mater. Sci. **2022**, 201, 110864.

(31) Su, Y.; Wang, J.; Zou, Y. Machine Learning-Aided High-Throughput First-Principles Calculations to Predict the Formation Energy of μ Phase. ACS Omega **2023**, 8, 37317–37328.

(32) Majzoub, E. H.; Ozoliņš, V. Prototype electrostatic ground state approach to predicting crystal structures of ionic compounds: Application to hydrogen storage materials. Phys. Rev. B **2008**, 77, 104115, Publisher: American Physical Society.

(33) Ishikawa, T.; Miyake, T.; Shimizu, K. Materials informatics based on evolutionary algorithms: Application to search for superconducting hydrogen compounds. Phys. Rev. B **2019**, 100, 174506, arXiv:1908.00746 [cond-mat].

(34) Nouira, A.; Sokolovska, N.; Crivello, J.-C. CrystalGAN: Learning to Discover Crystallographic Structures with Generative Adversarial Networks. AAAI 2019 Spring Symposium on Combining Machine Learning with Knowledge Engineering. 2019; p 18, https://hal.archives-ouvertes.fr/hal-01902821.

(35) Xie, T.; Grossman, J. C. Crystal Graph Convolutional Neural Networks for an Accurate and Interpretable Prediction of Material Properties. Phys. Rev. Lett. **2018**, 120, 145301.

(36) Li, Y.; Chen, J.; Cai, P.; Wen, Z. An electrochemically neutralized energy-assisted low-cost acid-alkaline electrolyzer for energy-saving electrolysis hydrogen generation. J. Mater. Chem. A **2018**, 6, 4948–4954.

(37) Sultanov, A.; Crivello, J.-C.; Rebafka, T.; Sokolovska, N. Data-Driven Score-Based Models for Generating Stable Structures with Adaptive Crystal Cells. J. Chem. Inf. Model. **2023**, 63, 6986–6997.

(38) Zeni, C.; Pinsler, R.; Zügner, D.; Fowler, A.; Horton, M.; Fu, X.; Wang, Z.; Shysheya, A.; Crabbé, J.; Ueda, S.; Sordillo, R.; Sun, L.; Smith, J.; Nguyen, B.; Schulz, H.; Lewis, S.; Huang, C.-W.; Lu, Z.; Zhou, Y.; Yang, H.; Hao, H.; Li, J.; Yang, C.; Li, W.; Tomioka, R.; Xie, T. A generative model for inorganic materials design. Nature **2025**, 1–3, Publisher: Nature Publishing Group.

(39) Oganov, A. R.; Glass, C. W. Crystal structure prediction using ab initio evolutionary techniques: Principles and applications. J. Chem. Phys. **2006**, 124, 244704.

(40) Lyakhov, A. O.; Oganov, A. R.; Stokes, H. T.; Zhu, Q. New developments in evolutionary structure prediction algorithm USPEX. Comput. Phys. Commun. **2013**, 184, 1172–1182.

(41) Falls, Z.; Avery, P.; Wang, X.; Hilleke, K. P.; Zurek, E. The XtalOpt Evolutionary Algorithm for Crystal Structure Prediction. J. Phys. Chem. C **2021**, 125, 1601–1620.

(42) Wang, Y.; Lv, J.; Zhu, L.; Ma, Y. CALYPSO: A method for crystal structure prediction. Comput. Phys. Commun. **2012**, 183, 2063–2070.

(43) Oganov, A. R.; Chen, J.; Gatti, C.; Ma, Y.; Ma, Y.; Glass, C. W.; Liu, Z.; Yu, T.; Kurakevych, O. O.; Solozhenko, V. L. Ionic high-pressure form of elemental boron. Nature **2009**, 457, 863–867.

(44) Wang, Z.; Zhou, X.-F.; Zhang, X.; Zhu, Q.; Dong, H.; Zhao, M.; Oganov, A. R. Phagraphene: A Low-Energy Graphene Allotrope Composed of 5–6–7 Carbon Rings with Distorted Dirac Cones. Nano Lett. **2015**, 15, 6182–6186, PMID: 26262429.

(45) Zhou, D.; Semenok, D.; Galasso, M.; Alabarse, F. G.; Sannikov, D.; Troyan, I. A.; Nakamoto, Y.; Shimizu, K.; Oganov, A. R. Raisins in a Hydrogen Pie: Ultrastable Cesium and Rubidium Polyhydrides. Adv. Energy Materi. **2024**, 14, 2400077.

(46) Glass, C. W.; Oganov, A. R.; Hansen, N. USPEX—Evolutionary crystal structure prediction. Comput. Phys. Commun. **2006**, 175, 713–720.

(47) Zhu, Q.; Oganov, A. R.; Glass, C. W.; Stokes, H. T. Constrained evolutionary algorithm for structure prediction of molecular crystals: methodology and applications. Acta Crystallogr. Sect. B **2012**, 68, 215–226.

(48) Bushlanov, P. V.; Blatov, V. A.; Oganov, A. R. Topology-based crystal structure generator. Comput. Phys. Commun. **2019**, 236, 1–7.

(49) Kresse, G.; Furthmüller, J. Efficiency of ab-initio total energy calculations for metals and semiconductors using a plane-wave basis set. Comput. Mater. Sci. **1996**, 6, 15–50.

(50) Kresse, G.; Furthmüller, J. Efficient iterative schemes for ab initio total-energy calculations using a plane-wave basis set. Phys. Rev. B **1996**, 54, 11169–11186.

(51) Perdew, J. P.; Burke, K.; Ernzerhof, M. Generalized Gradient Approximation Made Simple. Phys. Rev. Lett. **1996**, 77, 3865–3868.

(52) Monkhorst, H. J.; Pack, J. D. Special points for Brillouin-zone integrations. Phys. Rev. B **1976**, 13, 5188–5192.

(53) Hamada, I. van der Waals density functional made accurate. Phys. Rev. B **2014**, 89, 121103.

(54) Tran, F.; Kalantari, L.; Traoré, B.; Rocquefelte, X.; Blaha, P. Nonlocal van der Waals functionals for solids: Choosing an appropriate one. Phys. Rev. Mater. **2019**, 3, 063602.

(55) Togo, A.; Chaput, L.; Tadano, T.; Tanaka, I. Implementation strategies in phonopy and phono3py. J. Phys. Condens. Matter **2023**, 35, 353001.

(56) Togo, A. First-principles Phonon Calculations with Phonopy and Phono3py. J. Phys. Soc. Jpn. **2023**, 92, 012001.

(57) Krukau, A. V.; Vydrov, O. A.; Izmaylov, A. F.; Scuseria, G. E. Influence of the exchange screening parameter on the performance of screened hybrid functionals. J. Chem. Phys. **2006**, 125, 224106.

(58) Henkelman, G.; Arnaldsson, A.; Jónsson, H. A fast and robust algorithm for Bader decomposition of charge density. Comput. Mater. Sci. **2006**, 36, 354–360.

(59) Miwa, K.; Ohba, N.; Towata, S.-i.; Nakamori, Y.; Orimo, S.-i. First-principles study on lithium borohydride $LiBH_4$. Phys. Rev. B **2004**, 69, 245120.

(60) Ge, Q. Structure and Energetics of LiBH4 and Its Surfaces:A First-Principles Study. J. Phys. Chem. A **2004**, 108, 8682–8690, Publisher: American Chemical Society.

(61) Huang, X.; Duan, D.; Li, X.; Li, F.; Huang, Y.; Wu, G.; Liu, Y.; Zhou, Q.; Liu, B.; Cui, T. High-pressure polymorphism as a step towards high density structures of LiAlH4. Appl. Phys. Lett. **2015**, 107, 041906.

(62) Chase, M. NIST-JANAF Thermochemical Tables, 4th Edition; American Institute of Physics, Table 2, 1998; Vol. 1.

(63) Smith, M. B.; Bass, G. E. J. Heats and Free Energies of Formation of the Alkali Aluminum Hydrides and of Cesium Hydride. J. Chem. Eng. Data **1963**, 8, 342–346.

(64) Zhang, Y.; Wang, Y.; Michel, K.; Wolverton, C. First-principles insight into the degeneracy of ground-state $LiBH_4$ structures. Phys. Rev. B **2012**, 86, 094111.

(65) Miwa, K.; Aoki, M.; Noritake, T.; Ohba, N.; Nakamori, Y.; Towata, S.-i.; Züttel, A.; Orimo, S.-i. Thermodynamical stability of calcium borohydride $Ca(BH_4)_2$. Phys. Rev. B **2006**, 74, 155122.

(66) Majzoub, E. H.; Rönnebro, E. Crystal Structures of Calcium Borohydride: Theory and Experiment. J. Phys. Chem. C **2009**, 113, 3352–3358.

(67) Rude, L. H.; Filinchuk, Y.; Sørby, M. H.; Hauback, B. C.; Besenbacher, F.; Jensen, T. R. Anion Substitution in $Ca(BH_4)_2$-CaI_2: Synthesis, Structure and Stability of Three New Compounds. J. Phys. Chem. C **2011**, 115, 7768–7777.

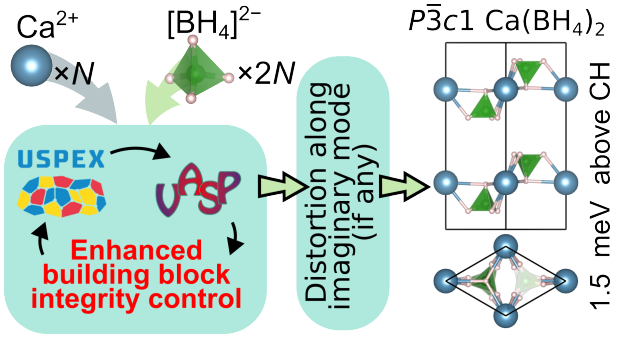

For Table of Contents Only